Many-body effects in the electronic spectra of cubic boron nitride

Guido Satta and Giancarlo Cappellini
INFM-Sardinian Laboratory for Computational Materials Science and Dipartimento di Fisica, Università di Cagliari, Cittadella Universitaria, Strada Prov.le Monserrato-Sestu Km 0.700, I-09042 Monserrato (Ca), Italy

Valerio Olevano and Lucia Reining
Laboratoire des Solides Irradiés UMR 7642, CNRS-CEA/DSM, École Polytechnique, F-91128 Palaiseau, France
(Received 14 March 2004; revised manuscript received 26 July 2004; published 18 November 2004)

We present state of the art first-principles calculations of optical spectra and the loss function of bulk cubic boron nitride (*c*-BN), starting from a density functional Kohn-Sham band structure. We investigate the influence of many-body effects beyond the random phase approximation (RPA) on the optical spectra through the inclusion of self-energy and excitonic effects by a GW calculation and the solution of the Bethe-Salpeter equation. For the loss function we only perform RPA calculations, since Bethe-Salpeter results are already available in the literature. We show to which extent, and in which kind of spectra, the description of many-body effects is important for a meaningful comparison with experiment, and when they can be neglected due to mutual cancellation. We also present results obtained within time-dependent density functional theory, both in the adiabatic local density approximation (TDLDA) and using a recently proposed long-range approximation for the exchange-correlation kernel. Our results show that the latter corrects a big part of the error with respect to RPA or TDLDA; however, the corrections are not sufficient to qualify the method for further quantitative predictions, in particular for the study of the optical gap. In fact, since experiments often quote a relatively low (around 6.4 eV) band gap, whereas the calculated optical absorption spectrum already in the random-phase approximation appears blueshifted by more than 2 eV with respect to the available experimental curve, we study in particular the question of the optical gap in this material. It turns out that, although there is evidence for a weakly bound exciton in *c*-BN, the optical gap of pure monocrystalline cubic BN should be around 11 eV, hence significantly bigger than has sometimes been quoted from experiments.

DOI: 10.1103/PhysRevB.70.195212 PACS number(s): 71.35.−y, 79.20.Uv, 71.10.−w, 71.45.Gm

I. INTRODUCTION

Boron nitride (BN) is a compound that has attracted considerable interest. Among other characteristics BN is known for its peculiar electronic and mechanical properties. Its hardness, high melting point and large bulk modulus make it ideal as protective coating material.[1,2] Besides this, other properties such as the high thermal conductivity, wide band gap and low dielectric constant, make BN very attractive for applications in optical and electronic devices.[1–3] In fact, nitride semiconductors are visible light emitters and detectors, and they have therefore gained importance due to already existing or potential applications. Many advanced technologies rely on boron nitride and on materials based on it, due to the wide spectrum of properties offered by its polymorphic modifications, two graphitelike and two dense ones. Moreover boron nitride shares many of its properties, structures, processings and applications with carbon.[1,2] Its physical properties, such as extreme hardness, wide energy band gap, low dielectric constant and high thermal conductivity, are also very near to those of diamond. Moreover, the possibility to grow BN nanotubes has stimulated a large interest upon the layered hexagonal phase (*h*-BN).[4]

These properties of boron nitride have motivated detailed theoretical and experimental studies for a long time.[5–7] Experimentally, bulk cubic BN (*c*-BN) is the thermodynamically stable phase at standard conditions, and the less dense *h*-BN becomes stable at high temperatures.[8] *c*-BN chemical vapor deposited films have been realized,[9] but the production of pure *c*-BN thin films remains a difficult task due to the formation, during the growth process, of undesired *h*-BN domains.[10] The minimum experimental band gap is direct in the case of *h*-BN, and indirect in the case of *c*-BN. For *h*-BN a direct band gap of 5.2 ± 0.2 eV associated with the transition H_{3v}-H_{2c} has been estimated,[11] while a value of 6.4 ± 0.5 eV for the indirect minimum band gap in *c*-BN has been inferred from experiment,[12] and associated with the Γ_{15v}-X_{1c} transition.[13] However, the value of 6.4 ± 0.5 eV has also often been associated with the optical absorption onset; in fact experimental spectra like transmission[12] or absorption (obtained from reflectance via a Kramers-Kronig transformation)[14] show structure starting roughly at that energy. For example, Miyata *et al.*[15] presented, on the basis of reflectance and transmission measurements, the complex refractive index for *c*-BN reporting an onset for absorption of 6.1 ± 0.5 eV, whereas Chen *et al.*,[16] measuring samples constituted of BN films with up to 88% of cubic phase, could conclude that the onset should be somewhere above 6.0 eV.

The experimental result of Osaka *et al.*,[14] where an optical absorption onset at 6.8 eV was estimated, has been addressed in many theoretical papers. Xu and Ching with an OLCAO method,[17] Christensen and Gorczyca in a LDA-LMTO scheme,[18] Gavrilenko and Wu with a FLAPW code,[19] all found that the DFT-LDA imaginary part of the macroscopic dielectric function, $\varepsilon_2(\omega)$, results blueshifted with respect to the curve of Ref. 14. This finding has also been confirmed by two of us in an earlier work: using a DFT-LDA code based

on pseudopotentials and plane waves, we have found an onset energy of 8.9 eV for the calculated $\varepsilon_2(\omega)$.[20] This value has been found also more recently by Ramos *et al.*,[21] using FLAPW and including relativistic corrections. The comparison between theoretical and experimental results for the absorption spectrum of this material appears singular in view of the fact that usually, due to the so-called *band-gap problem* for semiconductors and insulators, the DFT-LDA calculated absorption onset results redshifted with respect to the experimental one.[22–24] In Ref. 20 different possible explanations, ranging from lattice parameter mismatch to the presence of *h*-BN domains have been considered to explain the *inverse band-gap problem* for *c*-BN, without being successful. In fact, it is not possible to draw quantitative conclusions on the basis of RPA calculations alone, since they are well known to yield absorption spectra that can be far from the experimental ones. On top of a more or less rigid blueshift due to self-energy corrections, strong excitonic effects can modify the spectral line shapes and transition energies, in particular for insulators like BN.[22]

The question of many-body effects in the spectra of *c*-BN has already been addressed by other authors. The electron addition and removal (quasiparticle) energies of *c*-BN have been calculated for the first time by Suhr and co-workers,[13] using the GW approximation for the electron self-energy[25] on top of a DFT ground state calculation. The authors obtained for the direct gap at Γ a value of 11.4 eV, which they have compared to the peak near 14.5 eV found by Philipp and Taft[7] in an earlier work. (Those experimental data for *c*-BN had however been presented as marginal results, only meant to support the evidence for a larger direct band gap in *c*-BN than in diamond.[7]) There is also one published calculation that includes the electron-hole interaction:[26] nonresonant inelastic x-ray scattering (IXS) measurements were compared to calculations based on the solution of the Bethe-Salpeter equation, for various values and directions of the momentum transfer, showing good agreement between the experimental and the measured curves. In the same work, also the optical reflectance spectrum was calculated and compared to the measurements of Miyata *et al.*[15] The theoretical spectrum showed no structure around 6–7 eV, and the experimentally observed feature at that energy was therefore attributed to phonon-assisted transitions.

The Bethe-Salpeter approach has hence been shown to give a very good description of the excitation properties of cubic boron nitride, over a wide range of energies and momentum transfer. Nevertheless, on the basis of the results available in literature, several interesting questions still remain to be answered, namely: (i) the value of the optical gap has still to be definitely confirmed (it is not directly addressed in Ref. 26); (ii) it would be interesting to discuss the effect of the electron-hole interaction more in detail; in particular, whether a bound exciton shows up in this material; (iii) excitonic effects might have a different influence on the various optical constants (reflectance, transmission, refractive index, extinction coefficient, absorption); no systematic study about this question has been published to our knowledge, neither for BN nor for other semiconductors or insulators; (iv) Bethe-Salpeter calculations are cumbersome, and it would be interesting to see to which extent cancellation effects between the self-energy and the excitonic effects can be used to justify the much simpler RPA calculations; this is in particular reasonable to suppose in the case of the loss functions for small momentum transfer;[27] (v) when electron-hole effects have to be included, their effect may be reproduced also in time-dependent density functional theory, if a suitable independent-particle response function χ_0 and exchange-correlation kernel f_{xc} are used. A simple long-range approximation for f_{xc} (LRC), together with a χ_0 constructed using LDA wave functions but quasiparticle energies, has been shown[28,29] to yield excellent results for various small- and large-gap semiconductors. It is worthwile to try this approach for BN, because the LRC calculations are not more demanding than those performed in RPA, and this approach might allow one to deal with more complicated phases like mixed cubic/hexagonal ones.

In the present work, we address these questions. Using the above mentioned various state-of-the-art *ab initio* techniques, we can claim to have determined the intrinsic spectra of pure cubic BN, and to be able to assess to which extent discrepancies between theory and experiment may be attributed to deviations of the real samples from ideal *c*-BN ones. For the electron energy-loss spectra (EELS) we have limited the calculations to the random-phase approximation (RPA) including crystal local-field effects, since Galambosi *et al.*[26] have shown a large set of Bethe-Salpeter results, that we can use for comparison. Looking at our results it turns indeed out that RPA calculations (which are not given in Ref. 26) essentially yield spectra close to the Bethe-Salpeter ones. On the other hand, for the calculation of the macroscopic dielectric function we included, besides the local-field effects, both self-energy and excitonic effects through the solution of the Dyson and the Bethe-Salpeter (BSE) equations.[30] We found a result close to that of Ref. 26 for the reflectance spectrum, and we can show important excitonic effects also in the other optical constants. In particular, a bound exciton can be seen in the absorption spectrum. This effect could not be reproduced by the LRC approach, although the latter leads to an overall considerable improvement of the optical constants with respect to the RPA ones.

The paper is organized as follows: In Sec. II we present computational details of the ground-state calculation of *c*-BN and the corresponding results. In Sec. III we describe the theoretical schemes used to evaluate the optical constants and the loss function. In Sec. IV the resulting spectra are discussed and compared to other theoretical and experimental data. Finally, conclusions are drawn in Sec. V.

II. GROUND STATE CALCULATIONS

The ground-state calculation has been carried out within density-functional theory in the local-density approximation (LDA).[31] As exchange-correlation functional we used the Perdew and Zunger parametrization[32] of the Ceperley and Alder results.[33] Kohn-Sham orbitals are expanded in a plane waves basis and pseudopotentials have been used to represent the ion cores.[34,35] Separable, norm-conserving soft pseudopotentials have been generated within the scheme of

TABLE I. Lattice parameter dependence on the energy cutoff and the BZ sampling. In the first row values of a (in atomic units) are calculated using a set of 2 k-points in the irreducible BZ, while 10 k-points are used for the second row. In the first column the cut-off is 55 Rydberg while the results in the second one have been obtained with 70 Rydberg.

a (a.u.)	55 Ryd	70 Ryd
2 k	6.728	6.738
10 k	6.738	6.738

Troullier and Martins,[36] details relative to the choice of ionic pseudopotentials have been given in a previous pubblication.[20]

The results for the structural properties have been obtained thanks to the use of the ABINIT code[37] that relies on an efficient Fast-Fourier transform library[38] and a conjugate gradients algorithm.[39,40] Safe values could be chosen for all parameters that govern the numerical precision, since there are only 2 atoms per unit cell; in fact, all the calculations which are presented here, including the spectra below, have been performed on a personal computer platform P4 Intel (1.7 GHz and 1.5 Gbytes RAM).

In Table I we present the study of the convergence of the lattice parameter a with respect to the energy cutoff and the number of k-points used to represent the integrals in the first Brillouin zone (BZ). From the data of Table I the use of an energy cutoff of 55 Rydberg and of a set of 10 k points[41] in the irreducible wedge appear safe and stable. The maximum deviation of the values reported in Table I is 0.16% in modulo.

In Table II we have reported the results for the lattice parameter a and the bulk modulus B obtained by the present work in comparison with previous theoretical and experimental results.[42,43] The experimental value of the lattice parameter of c-BN has been determined with high accuracy (i.e., with an error bar of only 0.06%) by Knittel and co-workers.[43] In the present work we found a deviation of the theoretical lattice parameter from the experimental one of −1.4%. A detailed analysis of the dependence of the optical spectra upon lattice parameter variations has been given previously.[20] In that work it has been demonstrated that these variations could not explain the difference between theoretical and experimental optical absorption spectra.[19,20] Of course, excitonic effects might be influenced differently by the lattice parameter than the RPA spectra considered in those works, but the results presented below are such that any surprise can be safely excluded, and we do not pursue this point further.

TABLE II. Lattice parameters and bulk moduli for c-BN in comparison with previous results. In the first column after Ref. 20; in the second one those after Ref. 44; in the third one the present results; the fourth column reports the measured results after Refs. 42 and 43.

c-BN	Ref. 20	Ref. 44	Present	Expt.
a (a.u.)	6.754	6.759	6.738	6.833
B (Mbar)	4.01	3.97	4.03	3.68–4.65

III. CALCULATION OF OPTICAL AND ENERGY LOSS SPECTRA: THEORY AND COMPUTATIONAL APPROACH

The state-of-the-art approach to the calculation of optical absorption spectra of solids relies on the use of Green's functions methods: self-energy effects and the electron-hole attraction are explicitly included in the calculations. This can be done using the Bethe-Salpeter equation approach.[22,45,46] In the BSE approach, the macroscopic dielectric function reads

$$\varepsilon_M(\omega) = 1 + 2 \lim_{\mathbf{q}\to 0} v(\mathbf{q}) \sum_{\lambda} \frac{\left|\sum_{vc\mathbf{k}} \langle \phi_{v\mathbf{k}'} | e^{-i\mathbf{q}r} | \phi_{c\mathbf{k}} \rangle A_{\lambda}^{(vc\mathbf{k})}\right|^2}{E_{\lambda} - \omega - i\eta}, \tag{1}$$

where $v(\mathbf{q})$ is the bare Coulomb potential, $\mathbf{q}$ is a vector in the first Brillouin zone; $\phi_{n\mathbf{k}}$ are the Kohn-Sham wave functions; E_{λ} and $A_{\lambda}^{(vc\mathbf{k})}$ are the eigenvalues and eigenvectors of the excitonic Hamiltonian $\overline{H}^{\text{exc}}$ (we limit ourselves to the resonant contribution and to the static approximation for the electron-hole interaction), representing, respectively, the excitation energies of the system and the excitonic wave functions. Spin has been summed over. $\overline{H}^{\text{exc}}$ is given by

$$\overline{H}^{\text{exc}}_{(vc\mathbf{k})(v'c'\mathbf{k}')} = (\epsilon_{c\mathbf{k}} - \epsilon_{v\mathbf{k}})\delta_{vv'}\delta_{cc'}\delta_{\mathbf{kk}'} + i\overline{\Xi}_{(vc\mathbf{k})(v'c'\mathbf{k}')}, \tag{2}$$

where $\epsilon_{n\mathbf{k}}$ are the quasiparticle energies (as obtained, e.g., by the GW approximation) and $\overline{\Xi}_{(vc\mathbf{k})(v'c'\mathbf{k}')}$ is the representation in transition space of the static Bethe-Salpeter kernel

$$\overline{\Xi}(\mathbf{r}_1,\mathbf{r}_2,\mathbf{r}_3,\mathbf{r}_4) = -i\delta(\mathbf{r}_1,\mathbf{r}_2)\delta(\mathbf{r}_3,\mathbf{r}_4)\overline{v}(\mathbf{r}_1,\mathbf{r}_3) + i\delta(\mathbf{r}_1,\mathbf{r}_3)\delta(\mathbf{r}_2,\mathbf{r}_4)W(\mathbf{r}_1,\mathbf{r}_2), \tag{3}$$

where $\overline{v}$ is the Coulomb interaction without its long range term (this contribution reproduces the crystal local field effects), and W is the screened Coulomb interaction in the static RPA approximation.

In practice the Kohn-Sham (KS) eigenvalues and eigenfunctions from a DFT-LDA calculation serve as an input for the evaluation of the RPA screened interaction W and the GW self-energy Σ.[23,24,30] Then quasiparticle (QP) energies in the GW approximation are calculated, and these together with W are used as input for the evaluation of the Bethe-Salpeter kernel and the excitonic Hamiltonian, again calculated on the basis of (pairs of) KS wave functions. A diagonalization of the excitonic Hamiltonian gives the excitonic eigenvectors and eigenvalues used to evaluate the macroscopic dielectric function.

Alternatively, one can work in the framework of time-dependent density-functional theory (TDDFT). In contrast to the BSE approach, TDDFT is only involving 2-point response functions, and no 4-point quantities like e.g. Eq. (3),

which means that the computational effort is in principle strongly reduced.

The macroscopic dielectric function of a periodic system can be written as the inverse of the $\mathbf{G}=\mathbf{G}'=0$ element of the inverse microscopic dielectric matrix ($\mathbf{G},\mathbf{G}'$ are reciprocal lattice vectors)

$$\varepsilon_M(\omega) = \lim_{\mathbf{q}\to 0} \frac{1}{\varepsilon^{-1}_{\mathbf{G}=\mathbf{G}'=0}(\mathbf{q},\omega)}. \tag{4}$$

In TDDFT the microscopic dielectric matrix can be calculated through the matrix equation

$$\varepsilon^{-1} = 1 + v\chi^{(0)}(1-(v+f_{\mathrm{xc}})\chi^{(0)})^{-1}. \tag{5}$$

The exchange-correlation kernel f_{xc} is the functional derivative with respect to the density of the (in the general case, dynamical) Kohn-Sham exchange-correlation potential. The independent-particle polarizability $\chi^{(0)}$ is given by

$$\chi^{(0)}_{\mathbf{GG}'}(\mathbf{q},\omega) = 2\sum_{nn'\mathbf{k}} (f_{n\mathbf{k}} - f_{n'\mathbf{k}'}) \times \frac{\langle \phi_{n'\mathbf{k}'}|e^{-i\,(\mathbf{q}+\mathbf{G})\mathbf{r})}|\phi_{n\mathbf{k}}\rangle\langle\phi_{n\mathbf{k}}|e^{i\,(\mathbf{q}+\mathbf{G}')\mathbf{r}')}|\phi_{n'\mathbf{k}'}\rangle}{\epsilon_{n\mathbf{k}} - \epsilon_{n'\mathbf{k}'} - \omega - i\eta} \tag{6}$$

(here $\mathbf{k}'=\mathbf{k}+\mathbf{q}$, $\epsilon_{n\mathbf{k}}$ are the Kohn-Sham energies and $f_{n\mathbf{k}}$ are the occupation numbers; spin has been summed over).

In principle TDDFT should be able to correctly describe many-body effects in the optical and dielectric properties, provided that a good approximation for the exchange-correlation potential and its density variation, f_{xc}, is found. One possible choice is to set f_{xc} to 0, i.e., to neglect at all exchange-correlation effects in the response. This leads to the random-phase approximation, which does not at all take into account self-energy and excitonic effects; indeed it is known to be a rather crude approximation for optical spectra, at least when the LDA is used for the exchange-correlation *potential*, $v_{\mathrm{xc}}^{\mathrm{LDA}}$. Another widely used approximation is the so-called adiabatic local-density approximation (ALDA, also called TDLDA), which consists of taking as f_{xc} the functional derivative of the static exchange-correlation potential $v_{\mathrm{xc}}^{\mathrm{LDA}}$ in the local-density approximation, with respect to density. However, for absorption spectra of solids the use of the TDLDA generally leads to very similar results as the (unsatisfying) RPA.[22]

Recently it has been shown[22,28] that a long-range (LRC) tail in f_{xc} is capable of describing excitonic effects in semiconductors and some insulators. According to that scheme, a good approximation for f_{xc} is

$$f_{\mathrm{xc}}^{\mathrm{LRC}}(\mathbf{q},\mathbf{G},\mathbf{G}') = -\frac{\alpha}{|\mathbf{q}+\mathbf{G}|^2}\delta_{\mathbf{GG}'}, \tag{7}$$

where α is a parameter linearly related to the inverse of the dielectric constant $1/\varepsilon_\infty$. According to the law given in Ref. 29, corresponding to a calculated RPA value for the dielectric constant of *c*-BN of $\varepsilon_\infty=4.36$ [close to the experimental value of 4.5 (Ref. 47)], we find that α should be about 0.83. This method is computationally as efficient as the RPA, and has been shown to yield in different semiconductors and some insulators like SiC and diamond, good agreement both with theoretical results obtained within the BSE approach, and with the experimental ones. Therefore it could be a valid alternative to a full BSE calculation, which, due to computational limitations, cannot be applied to complex systems like e.g. disordered phases.

From the macroscopic dielectric function, one can derive the spectra we are interested in, for example the optical absorption [i.e., the imaginary part of ε_M, $\varepsilon_2(\omega)$], or the energy-loss function $-\mathrm{Im}(1/\varepsilon_M(\omega))$ for vanishing momentum transfer, as well as for a momentum transfer $\mathbf{q}+\mathbf{G}_0$, when $\mathbf{q}$ is taken to be finite and $\mathbf{G}=\mathbf{G}'=\mathbf{G}_0$ in Eq. (4).

Following Eqs. (3)–(5), in all our calculations, both in the BSE approach and in the TDDFT one, we have correctly taken into account local-field effects (LFE). This potentially important contribution[48] had been neglected in previous calculations of the loss function of *c*-BN,[17,20] but was of course included in Ref. 26, although the influence of LFE was not discussed explicitly in that reference.

Due to the slow convergence of optical calculations,[30] the macroscopic dielectric functions given here have been converged with a uniform mesh of 864 (shifted) *k*-points in the first Brillouin zone (BZ). In the case of the loss function we have used a 256 *k*-points mesh. The codes used were DP for the TDDFT calculations, and LSI-GW and EXC for the BSE approach.[49]

IV. OPTICAL CONSTANTS AND THE LOSS FUNCTION: RESULTS

We have first constructed the independent-particle response function χ_0 [Eq. (6)] using the Kohn-Sham band structure resulting from our ground state calculations. Of particular interest is the vertical transition energy across the gap at Γ, since it determines the onset of optical absorption when many-body effects are neglected and the transition is allowed. We find a value of 8.8 eV, close to Xu and Ching (Ref. 17: 8.7 eV) and to Suhr *et al.* (Ref. 13: 9.1 eV). This value is much bigger than the indirect gap Γ-*X*, for which we find 4.45 eV, i.e. a value between that of Suhr *et al.* (4.3 eV) and of Xu and Ching (5.18 eV). Concerning the small discrepancies, it is also worthwhile to note that our results are obtained for theoretical lattice constant while previous results are obtained by Suhr *et al.* and Xu and Ching both using the experimental lattice parameter (see also Table II). In any case, as pointed out above, the DFT-LDA KS direct gap turns out to be bigger than the often cited measured onset of optical absorption.

As it should be expected from the band structure, this leads to an optical spectrum that is blueshifted by about 2 eV with respect to the experimental one. Figure 1 shows the imaginary part of the macroscopic dielectric function calculated without the inclusion of LFE, i.e., directly from Eq. (6) (dotted-dashed line) which obviously well reproduces the previous result obtained by the two of us.[20] We have then included LFE through Eq. (4) (dotted line): although LFE are not completely negligible, they are by far not able to recover the discrepancy with the experiment of Osaka and

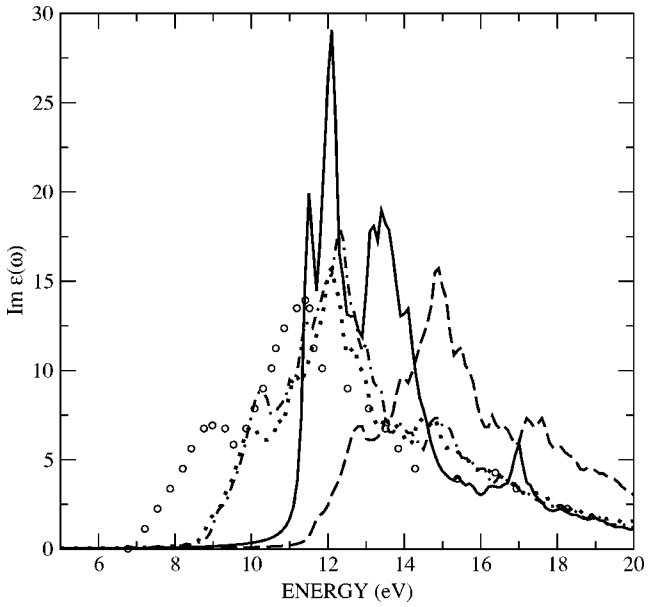

FIG. 1. Imaginary part of the macroscopic dielectric function of *c*-BN. Circles: experiment (Ref. 14); dotted-dashed line: LDA-RPA calculation, no LFE; dotted line: LDA-RPA, including LFE; dashed line: GW-RPA calculation including LFE; solid line: BSE calculation.

co-workers[14] (circles). Indeed, the present RPA with LFE result confirms the previous finding[17,20] concerning the overestimation of the theoretical optical onset (here 8.9 eV, associated with the Γ_{15v}-Γ_{15c} transition) with respect to the experiment [6.8 eV (Ref. 14)].

It is worthwhile to note two points: first, usually RPA spectra of insulators calculated using LDA Kohn-Sham eigenvalues appear to be redshifted with respect to the experiment. This is due to the well-known underestimation of the LDA Kohn-Sham energy-band gaps. In the present case an anomalous inverse band-gap problem seems to occur, i.e., LDA Kohn-Sham energy band gap overestimates the experiment. The second point is that here the RPA spectrum, apart from the unexplained blueshift, appears to reproduce the experimental main structures and globally the whole shape as presented by the experiment. We are indeed able to distinguish both in the experiment and in the RPA curve, a first modestly intense peak occurring just 2 eV after the onset, then the main peak at 4.5 eV again from the onset, followed by a shoulder at 6.5 eV and the last peak at 9.5 faraway from the onset. This could be taken as an indication of the fact that many-body effects, in particular electron-hole interaction effects, are of little relevance for the line shape. However, the big rigid shift of the spectrum would still have to be explained, and the similarity of the RPA and the measured spectra appears rather to be a coincidence, as it will be obvious later.

We have in fact gone beyond the LDA-RPA, and as a first step included GW corrections to the KS eigenvalues in the construction of χ_0 [Eq. (6)] in our calculations. The dashed line in Fig. 1 shows the result: since as usual the GW corrections are found to be positive[20,13] (they open the gap on average by about 2.85 eV), the GW-RPA curve is even further away from experiment than the LDA-RPA one. The GW optical onset is now shifted to 11.75 eV, close to the value of 11.4 found in the GW calculation of Ref. 13, again associated with the Γ_{15v}-Γ_{15c} transition, and the mismatch with the experimental onset raises to about 5 eV. The global shape of the spectrum is however not much changed.

Finally, with the solid line, we have reported the result obtained through a BSE calculation, i.e., including both self-energy and excitonic (electron-hole interaction) effects according to Eqs. (1)–(3). With respect to GW we find an important redistribution of oscillator strength towards lower energy. There is a strong intensification of the main peak, and the shoulder that was placed just at the right of it in the RPA results has become a clear peak. Also the distances between the structures are clearly affected. All these effects lead to a worsening of the agreement between theoretical and experimental line shapes. Concerning the value of the optical onset, not much improvement with respect to GW-RPA is obtained either: the BSE optical onset (corresponding to the first excitonic eigenvalue, and with oscillator strength that is visible in the optical spectrum) is placed at about 11.4 eV. We have hence indeed found a bound exciton, of relatively strong oscillator strength, but with a binding energy of only about 0.35 eV, which cannot counterbalance the GW shift of almost 3 eV. This result could seem to be a deception, but it is not suprising: using the calculated static dielectric constant of *c*-BN (ε_∞=4.4) and the effective mass tensor inferred from our bandstructure calculation, one can estimate, within the Wannier model, an exciton binding energy of roughly 0.3 eV. Further details that are included in the full *ab initio* calculations do not lead to spectacular changes of the exciton binding energy (although they are of course necessary in order to obtain good line shapes and quantitatively reliable spectra).

What we can now safely state is that a state-of-the-art calculated optical spectrum of pure cubic BN is far from the published experimental absorption spectrum. This assessment closes the series of works and discussions that have been dedicated to this point.

This unusual discrepancy should however not lead to hasty conclusions: it should neither be claimed that surprisingly a system has been found where the BSE scheme fails for the first time for this type of material, nor that measurements are simply wrong. Rather, one can first of all note that the optical absorption spectrum has never been measured directly, but always been derived from the reflectance measurements, using the Kramers-Kronig transformation. Since spectra are never measured on the whole frequency range, this procedure usually involves some hypothesis or modelling of the high-energy contributions.[15] Therefore, it is most instructive to go back to the curves that have originally been measured.

Figure 2 shows the comparison of calculated (upper panel) and measured (lower panel) reflectance spectra.

LFE turn out to have a minor effect (dotted as compared to dotted-dashed line), whereas GW corrections (dashed line) shift the reflectance spectrum rigidly to higher energies, essentially as it happens for absorption. The BSE result (continuous line) shows a one-to-one correspondence of structures with respect to the GW-RPA; each of these structures is

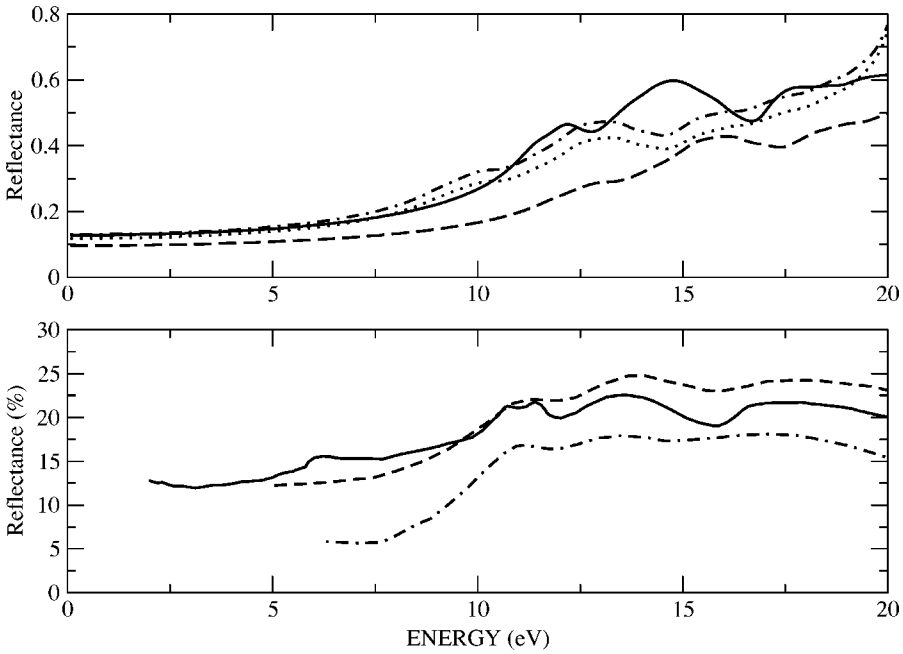

FIG. 2. Reflectance spectra of *c*-BN. Upper panel: calculations. Dotted-dashed line: LDA-RPA calculation, no LFE; dotted line: LDA-RPA, including LFE; dashed line: GW-RPA calculation including LFE; solid line: BSE calculation. Lower panel: experiments. Dashed line and dotted-dashed lines: results for sintered and microcrystalline samples, respectively, by Osaka *et al.* (Ref. 14) (arbitrary units); solid line: result of Miyata *et al.* (Ref. 15).

redshifted and enhanced by the electron-hole interaction. In contrast to absorption, it would be difficult to detect the presence of a bound exciton from the reflectance spectrum. More importantly, the agreement with the experimental spectrum of Miyata *et al.*[15] (solid line, lower panel) is good, except for the small structure that has been measured at about 6 eV and that is not present in the calculations. This finding confirms the comparison of Galambosi *et al.*,[26] who have shown a BSE reflectance spectrum (although calculated with a nonvanishing momentum transfer of 0.1 $Å^{-1}$). The comparison with the reflectance data of Osaka *et al.*[14] (dashed and dotted-dashed lines) is also fair, concerning the sintered sample maybe even better (note the absence of the 6 eV structure). It should be pointed out that Osaka *et al.*[14] have also measured reflectance of the hexagonal phase. The most prominent feature in those spectra is a strong peak at about 6 eV. Therefore, the presence of a small fraction of *h*-BN in the sample might be a possible explanation for the 6 eV feature found by Miyata *et al.*,[15] in contrast to the explanation by phonon-assisted transitions given by Galambosi *et al.*[26]

It would of course on the long term be desirable to be able to study directly more complex phases of BN, in particular mixtures of cubic and hexagonal contributions. Since this is not possible using the BSE approach, we have investigated the possibility of using the computationally much more efficient TDDFT-LRC scheme. This scheme has to be tested carefully, in particular since the presence of a bound exciton and the strong modifications of the line shape place *c*-BN in the vicinity of a material like MgO, where the TDDFT-LRC method has turned out to work moderately well.[29] It is hence not clear which result one can expect.

Figure 3 shows again the GW-RPA (dashed line) and BSE (solid line) results for the optical absorption, together with our TDLDA calculations (dotted line) and the results obtained with the TDDFT-LRC approach (dotted-dashed line). In contrast to TDLDA, indeed the TDDFT-LRC method removes most of the discrepancy between the RPA (or GW-RPA) and the BSE results: there is a strong shift of oscillator strength towards lower energies with respect to GW-RPA, leading to a significant increase of in particular the second, dominant peak (at about 12.7 eV in the TDDFT-LRC approach). Moreover, the first three structures are found within a range of about 2 eV both in BSE and in TDDFT-LRC (whereas the first three prominent structures in the RPA, GW-RPA, and TDLDA results are distributed over almost 5 eV). However, the effect is not quite strong enough, in particular concerning the increase of the first peak (that re-

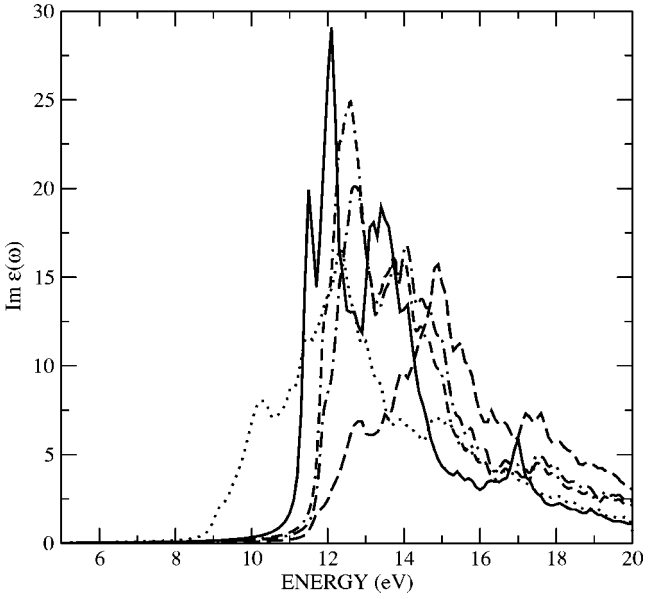

FIG. 3. Imaginary part of the macroscopic dielectric function of *c*-BN. Dotted-dashed line: TDDFT-LRC calculation with $\alpha=0.83$; dotted-double-dashed line: TDDFT-LRC calculation with $\alpha=1.0$; dotted line: TDLDA; dashed line: GW-RPA calculation including LFE; solid line: BSE calculation.

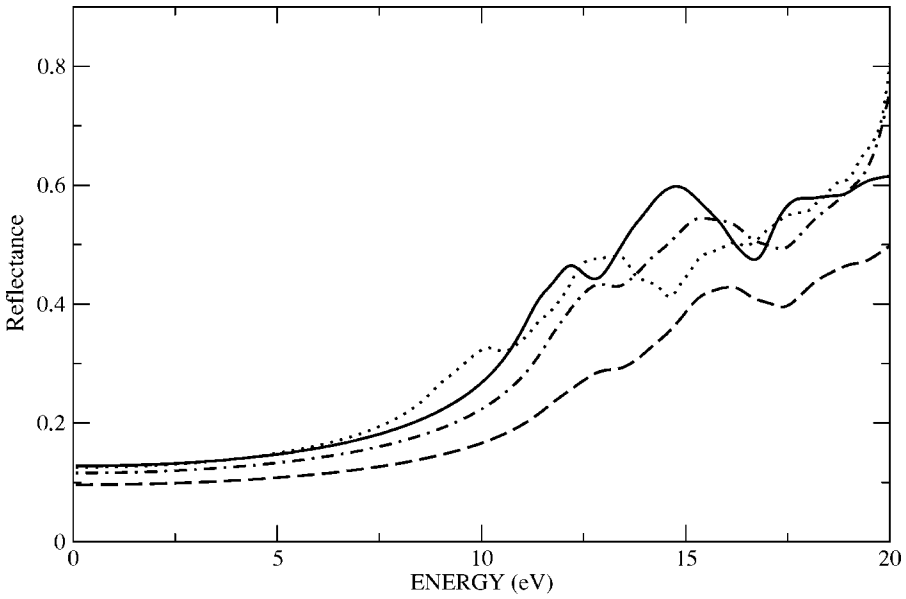

FIG. 4. Reflectance spectra of *c*-BN. Dotted-dashed line: TDDFT-LRC calculation; dotted line: TDLDA; dashed line: GW-RPA calculation including LFE; solid line: BSE calculation.

mains still a shoulder in TDDFT-LRC), and we moreover find an overall blueshift of about half an eV in the TDDFT-LRC result with respect to the BSE one. Of course, an increase of the parameter α from 0.83 to a higher value might improve the result. In fact, Fig. 3 also contains the result obtained with $\alpha=1.0$ (dotted-double-dashed curve) which is closer to the BSE result. However, if one wants to use this method in order to calculate a different, more complex, phase, α should not be treated as a fit parameter. Therefore, we can conclude that the TDDFT-LRC approach yields significant improvements with respect to the RPA, with a comparable computational effort, but that the results do not allow us to use this approach for exploring more complex phases in a fully quantitative and predictive way.

Figure 4 shows reflectance results, with a similar definition of the various curves as above for the absorption. Again we see a qualitative agreement of TDDFT-LRC calculation with BSE one in agreement with our previous conclusions for the dielectric function. However, since as pointed out above reflectance is not the good spectrum to use for the determination of a bound exciton, this is rather a way to hide, than to solve the problem.

The other optical constant that has been directly measured by Miyata *et al.*[15] is the transmittance. The experimental result is shown in the lower panel of Fig. 5; the curve shows a steep decrease starting from about 80% above 2 eV, a plateau at relatively low (about 15%) transmittance above 4 eV, and it falls to zero above 6.2 eV. The theoretical results, instead, are almost constant around 80% in that energy range, independently of the approximation that is used.

An explanation of this disagreement could come from the following conjecture if two hypotheses reveal true: (1) in the Miyata *et al.*[15] transmittance experiment it was used the same, with nonparallel surfaces, sample as in reflectance; (2)

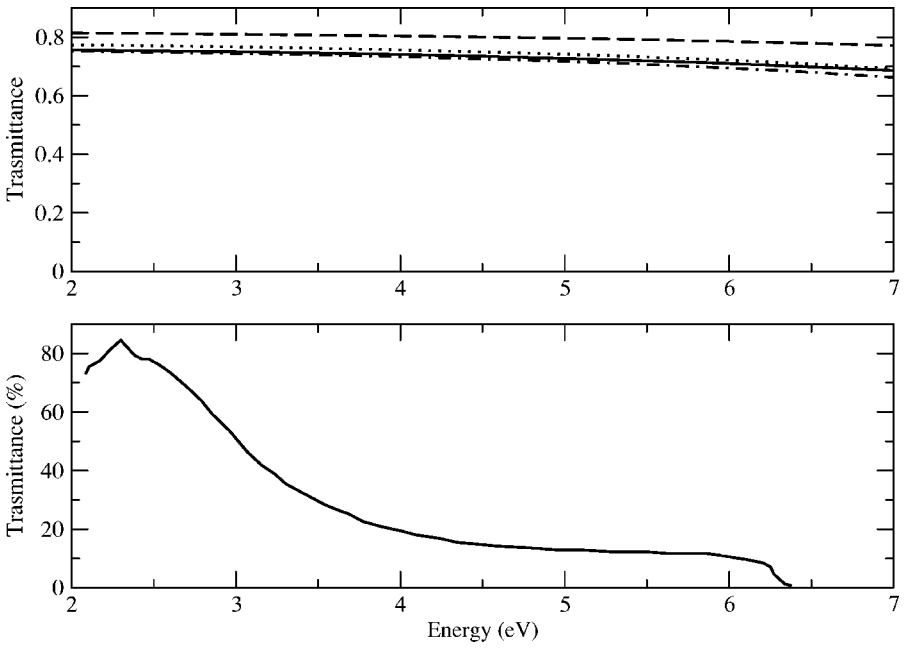

FIG. 5. Transmittance of *c*-BN. Upper panel: calculations. Dotted-dashed line: LDA-RPA calculation, no LFE; dotted line: LDA-RPA, including LFE; dashed line: GW-RPA calculation including LFE; solid line: BSE calculation. Lower panel: experiment by Miyata *et al.* (Ref. 15).

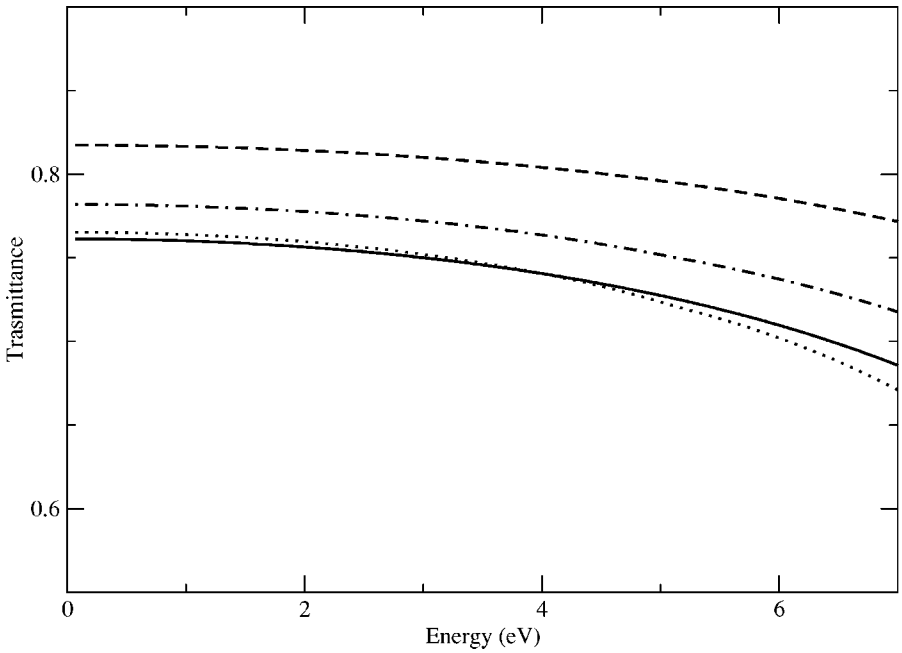

FIG. 6. Transmittance of *c*-BN. Dotted-dashed line: TDDFT-LRC calculation; dotted line: TDLDA; dashed line: GW-RPA calculation including LFE; solid line: BSE calculation.

the experimental setup was a *regular* (that is, not a *diffuse*) transmittance one; then, since regular transmittance is severely affected by the beam geometry, the measure out of the calibration point could be seriously affected by sample altered beam focusing. In fact, at the calibration point (2.10 eV, as reported in the text of Ref. 15) the experiment reports a value which is slight below 80%, that is more or less what is found by the theory.

The difference between the various approaches is essentially a rigid shift, with a slight divergence between the various curves towards higher energies.

Concerning the absolute values, their difference at 6 eV is still contained within 10%. The lowest result is obtained when RPA is used and LFE are neglected. When LFE are included, the result is very close to the BSE one, whereas GW-RPA yields a significantly higher value: this shows the strong cancellation effects between self-energy and electron-hole attraction effects on the transmittance. As can be seen in Fig. 6, this cancellation effect can be reproduced to a large extent by the TDDFT-LRC method (dotted-dashed curve). However, the deviation between TDDFT-LRC and the BSE result increases with increasing energy (up to 5% at 7 eV), whereas the RPA result stays close to the BSE one. TDLDA yields results that are in this case very close to the BSE ones.

Miyata *et al*. have used their reflectance and transmittance data in order to obtain other optical constants between 2 and 5.5 eV, and they have determined these functions for energies above 5.5 eV by using the measured reflectance together with a Kramers-Kronig transform (based indirectly on the low-energy transmittance data, through the use of a generalized mean-value theorem[50] for integrals). We have displayed their results in Figs. 7 and 9 (lower panels), together with our calculations (upper panels, and Figs. 8 and 10).

Let us first compare the full (BSE, continuous curve) result to experiment. The calculated curve for the refractive index *n* shows three prominent structures, at about 11.5, 13, and 17 eV. These structures can be identified with the double peak between 10.7 and 11.5 eV, the shoulder at about 13 eV, and the peak at about 16.5 eV in the experiment. Starting from a comparable plateau value (slightly above 2) the theoretical curve has much more pronounced structures, which might be due to the fact that calculations are carried out for a temperature equal to 0 K. A similar comparison holds for the extinction coefficient, *k*. The main difference between theory and experiment lies in both cases at the low-energy side, where in the experiment *n* has an additional peak at 6.3 eV, and *k* starts a slow rise at 6 eV; calculations do not yield this peak in *n*, and show a steep rise above 10 eV. Clearly, this discrepancy must have the same origin as the discrepancy found in the reflectance spectrum (from which the "experimental" optical constants were in fact obtained) and might therefore be due to the presence of hexagonal contributions.

Compared to the BSE and to experiment, the RPA shifts the structures to lower, the GW-RPA approximation to higher energies, and are both far from experiment. This is also true for the TDLDA (dotted line in Fig. 8). A rather good result is instead obtained by the LRC approach (dotted-dashed line in Fig. 8): about half of the error of the GW-RPA concerning peak positions is corrected and the strong enhancement of the first prominent peak due to the electron-hole interaction is correctly reproduced. The remaining error of the peak positions with respect to the BSE is probably due to the fact that, as pointed out above, the LRC approach does not correctly reproduce the bound exciton, although the latter cannot be detected as easily here as in the absorption spectrum.

The lower panel of Fig. 9 shows the experimental absorption coefficient. Like the extinction coefficient, it shows a slow rise above 6 eV followed by a steeper one above 10 eV, with three structures situated at about 11.5, 14, and above 17 eV. In correspondence, theory (BSE, continuous curve, upper panel) yields peaks at 12.2, 14.2, and 17.3 eV. Again, this good agreement is only obtained when the electron-hole interaction is included, fully through the BSE or partially in the LRC approach (dotted-dashed line, Fig.

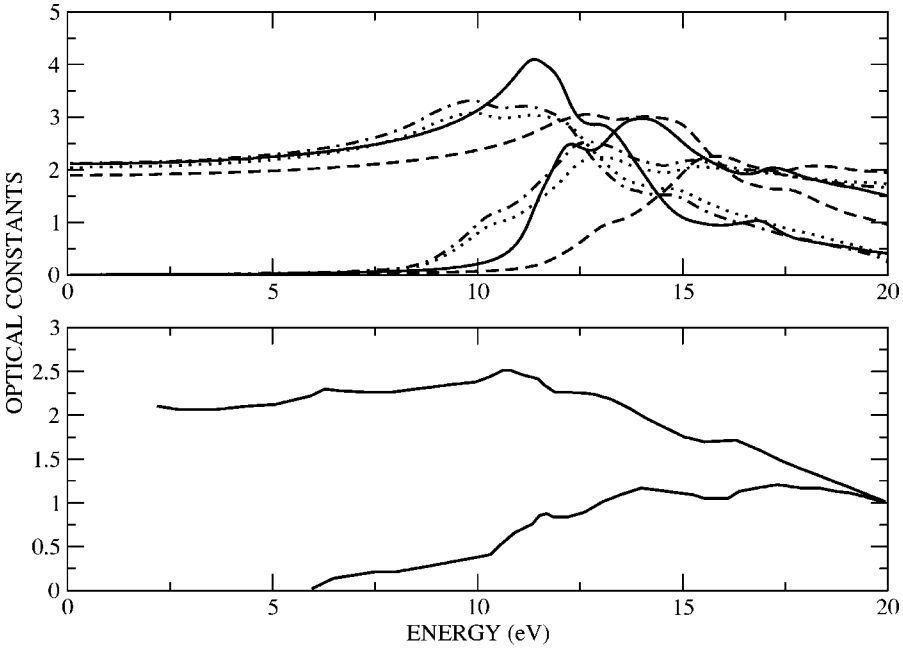

FIG. 7. Refractive index and extinction coefficient of *c*-BN. Upper panel: calculations. Dotted-dashed line: LDA-RPA calculation, no LFE; dotted line: LDA-RPA, including LFE; dashed line: GW-RPA calculation including LFE; solid line: BSE calculation. Lower panel: experiment by Miyata *et al.* (Ref. 15).

10), whereas the agreement obtained with the other approximations is much poorer.

A point that should be stressed for all the results presented above is the fact that the agreement between calculated results (within the BSE) and the data of Miyata *et al.*[15] is quite fair, much better than the comparison to the experimental absorption spectrum of Osaka *et al.*[14] However, the spectrum that was directly measured by Osaka and co-workers was the reflectance that, as shown above, was actually in fair agreement with the one measured by Miyata and co-workers. The absorption spectrum follows only indirectly from the measured data. We can therefore conclude that the absorption spectrum of Osaka *et al.*[14] is not the best choice for a comparison between theory and experiment, and that a detailed comparison of various optical constants shows much less disagreement, and is much less puzzling, than what could be deduced from earlier work.[20]

This analysis of the situation can be confirmed by further comparisons to existing independent experimental data. In fact, for finite momentum transfer Galambosi and co-workers[26] have found very good agreement between the loss function from nonresonant IXS experiments and calculations using the BSE. Here we compare our calculated RPA loss function to both these experimental and theoretical data,

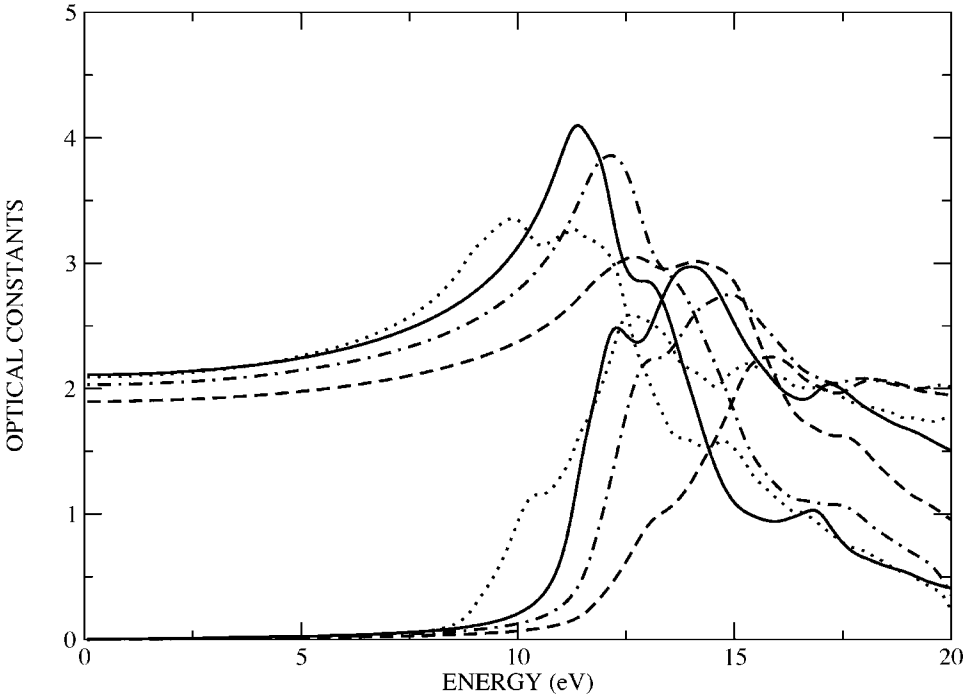

FIG. 8. Refractive index and extinction coefficient of *c*-BN. Dotted-dashed line: TDDFT-LRC calculation; dotted line: TDLDA; dashed line: GW-RPA calculation including LFE; solid line: BSE calculation.

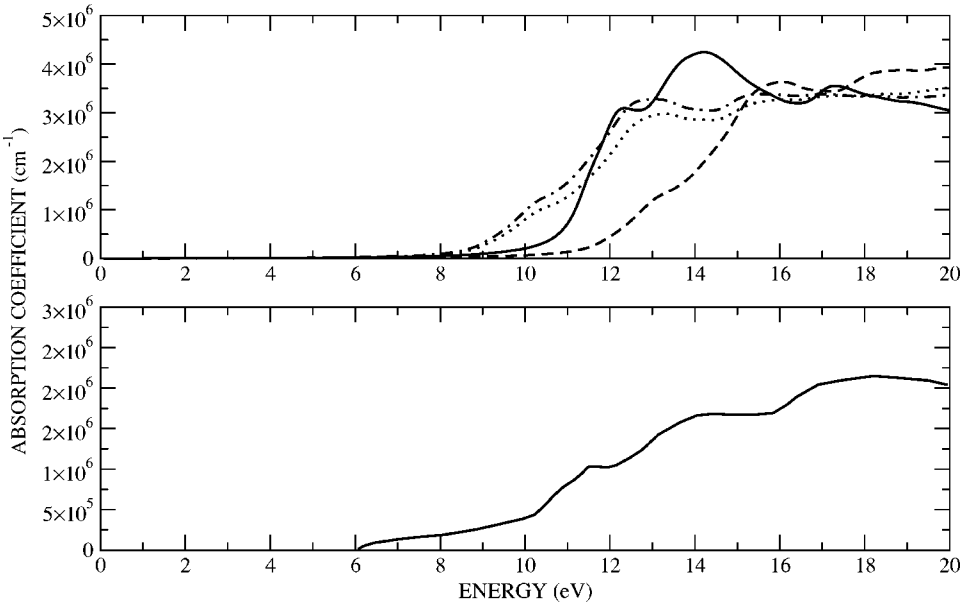

FIG. 9. Absorption coefficient of *c*-BN. Upper panel: calculations. Dotted-dashed line: LDA-RPA calculation; dotted line: LDA-RPA without LFE; dashed line: GW-RPA calculation including LFE; solid line: BSE calculation. Lower panel: experiment by Miyata *et al.* (Ref. 15).

with the aim to determine to which extent many-body effects have to be explicitly included in the calculation of inelastic x-ray scattering (IXS) spectra.

We have performed RPA calculations for various directions and values of the momentum transfer **q**, close to the values displayed in Fig. 1 of Ref. 26 The RPA results shown in Fig. 11 turn ideed out to be very good: in the Γ-X direction (left panel), we find in agreement with the BSE results and with experiment that with increasing momentum transfer the peak around 30 eV, that is rather compact for low momentum transfer (although 3 structures are resolved in the BSE and the RPA calculation), evolves into a two-peak structure for **q** around 0.5 ΓX. The distance between these two peaks increases when q is further increased, and a relatively flatter and extended shape is seen when q approaches $1\Gamma X$. Also the formation of an additional structure around 15 eV is correctly reproduced by the RPA. The main difference between the RPA and the BSE (and experimental) result is the fact that RPA slightly underestimates oscillator strength at lower energy. Positions are only slightly modified, and these discrepancies are clearly not big enough to prevent one to use RPA in order to interpret the experimental results. It should be noted that inclusion of local field effects is more important for increasing momentum transfer. It should also be stressed again that this does not imply that many-body effects are weak: GW corrections significantly shift the plasmon peaks [for example, by about 3 eV for **q** $0.5\Gamma X$ (Ref. 26)], but visibly the peaks are then shifted back by the electron-hole attraction, like in the case of silicon, for example.[51]

The situation is very similar in the ΓK and ΓL directions: in the first case, RPA correctly reproduces the trend with increasing momentum transfer towards the formation of a three-structures spectrum in the energy range considered.

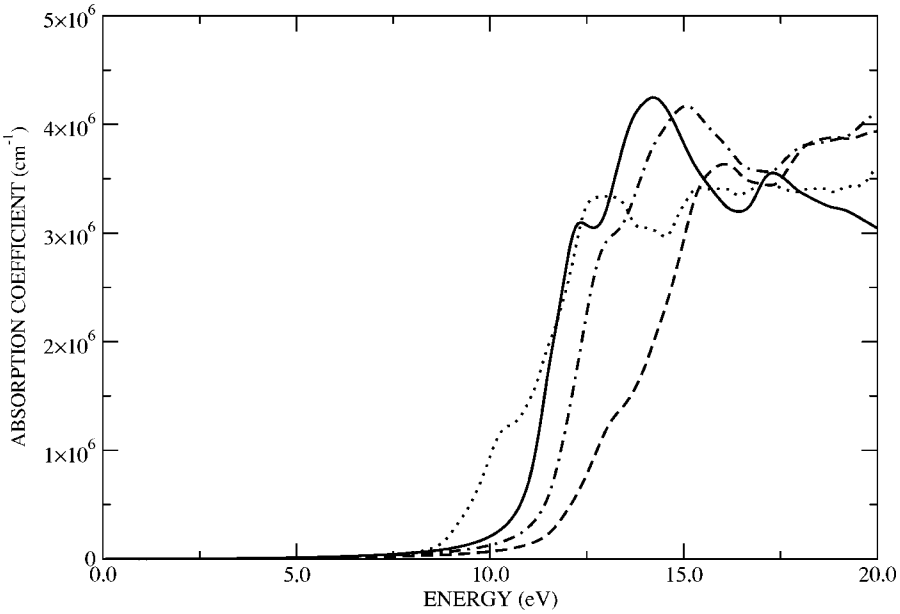

FIG. 10. Absorption coefficient of *c*-BN. Dotted-dashed line: TDDFT-LRC calculation; dotted line: TDLDA; dashed line: GW-RPA calculation including LFE; solid line: BSE calculation.

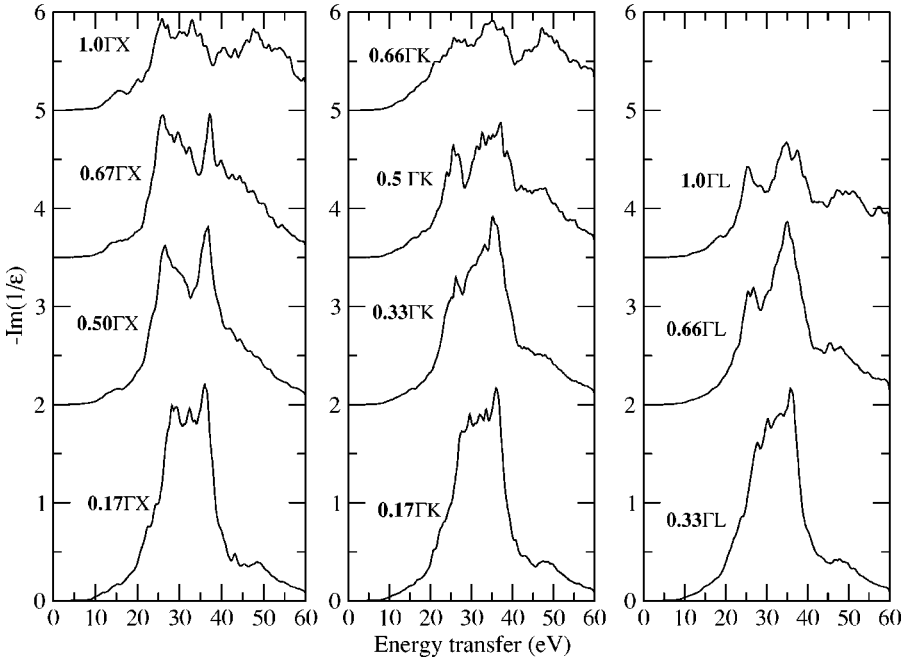

FIG. 11. Loss function of *c*-BN, results calculated using RPA including LFE, for various directions and absolute values of the momentum transfer.

Also the fact that the low-energy and the high-energy structures disperse to decreasing and increasing energy, respectively, is found in RPA. In direction Γ*L*, RPA describes in agreement with experiment the increase of the low-energy shoulder, whose position disperses less than the low-energy peak found in the Γ*K* direction. RPA also finds the additional weak feature showing up around 20 eV for q above $1\Gamma L$, as well as the formation of the broad shoulder around 50 eV.

This excellent agreement also allows us to discuss more critically the comparison to older experiments that was performed in previous works. In particular, the comparison of the energy-loss function of *c*-BN for vanishing momentum transfer between RPA results and the experimental data of McKenzie and co-workers[52] has been reported by Xu and Ching.[17] The experimental result showed one broad peak that did not resolve the three-peak structure found, as in the present work, by Xu and Ching,[17] and the overall weight was placed at lower energies than in the calculation. In fact, the experimental loss spectrum exhibits a broad peak centered at about 28.5 eV, which lies in the range of structures found both in the RPA calculation of the present work and of that in the work of Xu and Ching.[17] However, the line shapes differ considerably. In fact, the theoretical spectra consist of several peaks, and it is difficult to identify *the* plasmon frequency ω_p. One can resort to the definition $\mathrm{Re}(\varepsilon_M(\omega_p))=0$: in that case, as can be seen from Fig. 12, where we show the real (continuous curve) and imaginary (dashed curve) part of ε_M, as well as the loss function, we find about $\omega_p=29$ eV, which

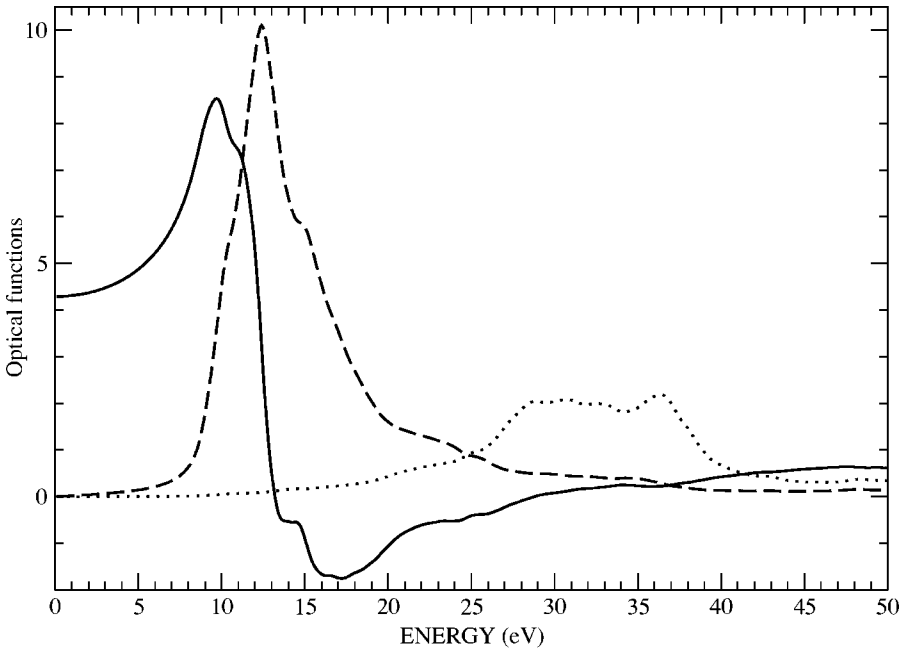

FIG. 12. Real (continuous line) and imaginary part (dashed line) of the macroscopic dielectric function, and loss function (dotted line) of *c*-BN. Results calculated using RPA including LFE, for vanishing momentum transfer.

corresponds to the first structure on the main plasmon peak. This value is not very far from the classical prediction for the plasma frequency in cubic BN (31 eV corresponding to an *ab initio* calculated $r_s = 1.32$). This indicates again that *c*-BN in itself does not exhibit any surprising spectacular features that would explain an unusual deviation between theory and experiment. On the other hand, the classical prediction for *h*-BN as well as inelastic electron scattering results[53] show that the total plasmon for the hexagonal phase is situated at lower energy (around 25 eV, depending on the direction of the momentum transfer). The fact that the experimental plasmon peak measured by McKenzie and co-workers[52] is found at lower energies than in the theoretical predictions and than in the IXS measurements[26] suggests again the possibility that the experimental sample used in Ref. 52 may contain contributions of the two phases.

In fact, at this point we can state that reliable theoretical results indicate that the samples measured in the various optical experiments are most probably not pure, monocrystalline cubic BN, but contain contributions from the hexagonal phase, a possibility that has already been suggested in previous theoretical[20] and experimental work.[54] As has been shown by other authors, for nonvanishing momentum transfer comparison between many-body theory and experiment is very good.[26] Our results presented here shows however that already a RPA calculation is precise enough to analyze energy-loss experiments: the inclusion of further many-body effects can be avoided since, as mentioned above, self-energy and excitonic effects tend to strongly cancel each other in the overall plasmon spectra (of course, the same statement would not be true if one zoomed on e.g., the interband transitions on the low-energy side of the loss peak).

V. CONCLUSIONS

Electronic and optical spectra of bulk cubic boron nitride have been calculated from first principles. Many-body interactions up to excitonic effects are included in the optical spectra using the GW approximation for the electron self-energy and the Bethe-Salpeter equation for the description of the electron-hole interaction. With respect to the RPA the self-energy corrections open the gap by about 5 eV, whereas the exciton binding energy is less than 0.4 eV. This increases the blueshift with respect to often cited experimental values for the absorption onset (above 6 eV). However, a careful analysis of several optical constants shows that calculations including the electron-hole interaction agree indeed well with experiment above 10 eV and suggest that below 10 eV contributions from the hexagonal phase show up. This is also suggested by the results for the loss function. Concerning theory, we have shown that already the RPA is sufficient for the description of the loss function even at relatively large momentum transfer, whereas all optical constants are well described only when the electron-hole interaction is taken into account, either through the solution of the Bethe-Salpeter equation or by using the TDDFT-LRC approach. In the latter case, calculations are as quick as in the case of RPA, and still reproduce the main features of the optical spectra. Only the exciton binding energy, of about 0.4 eV, is not obtained, which prevents this approach from being used for the determination of the optical gap in more complex phases of BN.

ACKNOWLEDGMENTS

This work has been supported in part by the European Community Contract No. HPRN-CT-2000-00167. The authors wish to aknowledge the use of the ABINIT simulation package (Ref. 37) to perform ground-state calculations presented here. TDDFT calculations have been done using the DP code and Bethe-Salpeter ones using the code EXC (Ref. 49). The authors would like to thank Maurizia Palummo and Giovanni Onida for many helpful discussions.

[1] *Synthesis and Properties of Boron Nitride*, edited by J.J. Pouch and S.A. Alterovitz (Trans. Tech. Publications, Aedermannsdorf, 1990).

[2] *Properties of Group III Nitrides*, edited by J.H. Edgar [Kansas State University (U.S.A.), Institute of Electrical Engineers, 1994].

[3] *Group III Nitride Semiconductors Compounds: Physics and Applications*, edited by B. Gil (Oxford Science Publications, London, 1998).

[4] X. Blase, A. Rubio, S.G. Louie, and M.L. Cohen, Europhys. Lett. **28**, 335 (1994).

[5] L. Kleinmann and J.C. Phillips, Phys. Rev. **117**, 460 (1960).

[6] E. Doni and G. Pastori Parravicini, Nuovo Cimento B **64**, 117 (1969).

[7] H.R. Philipp and E.A. Taft, Phys. Rev. **127**, 159 (1962).

[8] M.I. Eremets, K. Takemura, H. Yusa, D. Golberg, Y. Bando, V.D. Blank, Y. Sato, and K. Watanabe, Phys. Rev. B **57**, 5655 (1998).

[9] M. Sokolowski, J. Cryst. Growth **46**, 136 (1979).

[10] G. Kern, G. Kresse, and J. Hafner, Phys. Rev. B **59**, 8551 (1999).

[11] D.M. Hoffman, G. L. Doll, and P.C. Eklund, Phys. Rev. B **30**, 6051 (1984).

[12] R.M. Chrenko, Solid State Commun. **14**, 511 (1974).

[13] M. P. Surh, S. G. Louie, and M.L. Cohen, Phys. Rev. B **43**, 9126 (1991).

[14] Y. Osaka, A. Chayahara, H. Yokohama, M. Okamoto, T. Hamada, T. Imura, and M. Fujisawa, *Synthesis and Properties of Boron Nitride*, Materials Science Forum, edited by J.J. Pouch and S. A. Alteroviz (Trans. Tech Aedermanndorf, Switzerlad, 1990), Vols. 54 and 55, pp. 277–294.

[15] N. Miyata, K. Moriki, O. Mishima, M. Fujisawa, and T. Hattori, Phys. Rev. B **40**, 12 028 (1989).

[16] G. Chen, X. Zhang, B. Wang, X. Song, B. Cui, and H. Yan, Appl. Phys. Lett. **75**, 10 (1999).

[17] Y.-N. Xu and W.Y. Ching, Phys. Rev. B **44**, 7787 (1991).

[18] Christensen, Gorczyca, Phys. Rev. B **50**, 4397 (1994).

[19] V.I. Gavrilenko and R.Q. Wu, Phys. Rev. B **61**, 2632 (2000).

[20] G. Cappellini, G. Satta, M. Palummo, and G. Onida, Phys. Rev. B **64**, 035104 (2001).
[21] L.E. Ramos, L.K. Teles, L.M.R. Scolfaro, J.L.P. Castineira, A.L. Rosa, and J.R. Leite, Phys. Rev. B **63**, 165210 (2001).
[22] Giovanni Onida, Lucia Reining, and Angel Rubio, Rev. Mod. Phys. **74**, 601 (2002).
[23] M.S. Hybertsen and S.G. Louie, Phys. Rev. B **34**, 5390 (1986).
[24] R. W. Godby, M. Schlüter, and L. J. Sham, Phys. Rev. B **37**, 10 159 (1988).
[25] L. Hedin, Phys. Rev. **139**, 796 (1965); L. Hedin and S. Lundquist, in *Solid State Physics*, edited by H. Herenreich, F. Seitz, and D. Turnbull (Academic, New York, 1969), Vol. 23, p. 1.
[26] S. Galambosi, J.A. Soininen, K. Hämäläinen, E.L. Shirley, and C.-C. Kao, Phys. Rev. B **64**, 024102 (2001).
[27] Valerio Olevano and Lucia Reining, Phys. Rev. Lett. **86**, 5962 (2002).
[28] L. Reining, V. Olevano, A. Rubio, and G. Onida, Phys. Rev. Lett. **88**, 066404 (2002).
[29] Silvana Botti, Francesco Sottile, Nathalie Vast, Valerio Olevano, and Lucia Reining, Phys. Rev. B **69**, 155112 (2004).
[30] S. Albrecht, L. Reining, R. Del Sole, and G. Onida, Phys. Status Solidi A **170**, 189 (1998).
[31] R.M. Dreizler and E.K.U. Gross, *Density Functional Theory* (Spinger, New York, 1990).
[32] J.P. Perdew and A. Zunger, Phys. Rev. B **23**, 5048 (1981).
[33] D.M. Ceperley and B.J. Alder, Phys. Rev. Lett. **45**, 566 (1980).
[34] X. Gonze, R. Stumpf, and M. Scheffler, Phys. Rev. B **44**, 8503 (1991).
[35] M. Fuchs and M. Scheffler, Comput. Phys. Commun. **119**, 67 (1999).
[36] N. Troullier and J. L. Martins, Phys. Rev. B **43**, 1993 (1991).
[37] The ABINIT code is a common project of the Université Catholique de Louvain, Corning Incorporated, and other contributors (URL http://www.abinit.org).
[38] S. Goedecker, SIAM J. Sci. Comput. (USA) **18**, 1605 (1997).
[39] M.C. Payne, M.P. Teter, D.C. Allen, T.A. Arias, and J.D. Joannopoulos, Rev. Mod. Phys. **64**, 1045 (1992).
[40] X. Gonze, Phys. Rev. B **54**, 4383 (1996).
[41] D.J. Chadi and M.L. Cohen, Phys. Rev. B **8**, 5747 (1973).
[42] *Landolt-Börnstein: Numerical Data and Functional Relationships in Science and Technology*, edited by K.-H. Hellwege (Springer, New York, 1982), Group III, Vol. 17a.
[43] Elise Knittel, Renata M. Wentzcovitch, Raymond Jeanloz, and Marvin L. Cohen, Nature (London) **43**, 349 (1989).
[44] J. Furthmüller, J. Hafner, and G. Kresse, Phys. Rev. B **50**, 15 606 (1994).
[45] W. Hanke and L.J. Sham, Phys. Rev. Lett. **43**, 387 (1979).
[46] Michael Rohlfing and Steven G. Louie, Phys. Rev. Lett. **81**, 2312 (1998); **83**, 856 (1999).
[47] P.J. Gielisse, S.S. Mitra, J.N. Plendl, R.D. Griffis, L.C. Mansur, R. Marshall, and A.E. Pascoe, Phys. Rev. **155**, 1039 (1967).
[48] A.G. Marinopoulos, L. Reining, Valerio Olevano, Angel Rubio, T. Pichler, X. Liu, M. Knupfer, and J. Fink, Phys. Rev. Lett. **89**, 076402 (2002).
[49] DP and EXC codes, URL: http://theory.lsi.polytechnique.fr/codes/
[50] D.M. Roessler, J. Appl. Phys. **16**, 1119 (1965); **17**, 1313 (1966).
[51] V. Olevano and L. Reining, Phys. Rev. Lett. **86**, 5962 (2001).
[52] D.R. McKenzie, W.G. Sainty, and D. Green, *Synthesis and Properties of Boron Nitride*, Materials Science Forum, edited by J.J. Pouch and S.A. Alteroviz (Trans. Tech Aedermanndorf, Switzerland, 1990), Vols. 54 and 55, pp. 193–206.
[53] C. Tarrio and S.E. Schnatterly, Phys. Rev. B **40**, 7852 (1989).
[54] P. Widmayer, H.-G. Boyen, P. Ziemann, P. Reinke, and P. Oelhafen, Phys. Rev. B **59**, 5233 (1999).